Stable bound orbits in microstate geometries

Shinya Tomizawa[*] and Ryotaku Suzuki[†]

Mathematical Physics Laboratory, Toyota Technological Institute Hisakata 2-12-1, Nagoya 468-8511, Japan

(Received 30 March 2022; accepted 13 May 2022; published 8 June 2022)

We show the existence of stable bound orbits for the massive and massless particles moving in the simplest microstate geometry spacetime in the bosonic sector of the five-dimensional minimal supergravity. In our analysis, reducing the motion of particles to a two-dimensional potential problem, we numerically investigate whether the potential has a negative local minimum.

DOI: 10.1103/PhysRevD.105.124014

I. INTRODUCTION

The microstate geometries [1–14] are smooth horizonless solutions with the same asymptotic structure as a black hole or a black ring. So far, these solutions have been thought of as one of ways to resolve the problem of black hole information loss. The idea to describe black hole microstates by horizonless geometries first originated from the works on fuzzballs of Mathur [15–17]. The existence itself of such solutions should be surprising because in the earlier works [18–21], it is a well-known fact that smooth soliton solutions in four dimensions are completely excluded. However, in five dimensions, at least in five-dimensional supergravity, the no-go theorem does not hold because the spacetime admits the spatial cross sections with nontrivial second homology and the Chern-Simons interactions.

There are many ways to probe physical aspects of such microstate geometries. The simplest and most interesting way to probe the microstate geometries may be studying geodesic motion of massive and massless particles in such spacetimes. In particular, it is an interesting issue what is significantly different between the motion of particles (e.g., the existence/nonexistence of stable bound orbits) in microstate geometries and that in black hole spacetimes. Many researchers have so far studied particle motions in black hole spacetimes. For example, it is well known that in a four-dimensional Schwarzschild background, stable bound orbits exist for massive particles and do not exist for massless particles, whereas in a five-dimensional Schwarzschild background [22], they do not exist for both massive and massless particles. Moreover, stable bound orbits for rotating spherical black holes [23–26], black holes with nontrivial topologies [27–33], and Kaluza-Klein black holes [34,35] were also investigated. On the other hand, in supersymmetric microstate geometries [36,37], massless particles with zero energy are stably trapped on an evanescent ergosurface, which are defined as timelike hypersurfaces such that a stationary Killing vector field becomes null there and timelike everywhere except there.

As shown in Ref. [38], the angular momenta of the asymptotically flat, biaxisymmetric, reflectionally symmetric microstate geometries with a small number of centers (five centers) in the five-dimensional ungauged minimal supergravity have lower bounds, which are slightly smaller than those of the maximally spinning solutions of the Breckenridge-Myers-Peet-Vafa (BMPV) black holes [39] [asymptotically flat black holes with the mass and electric charge obeying the Bogomol'nyi-Prasad-Sommerfield (BPS) condition and equal angular momenta in the same theory]. This means that there exists a certain parameter region such as the microstate geometries with a small number of the centers that have the same angular momenta as the BMPV black holes. It is interesting to compare particle motion in the microstate geometries within such a parameter region with one in the black hole spacetime. For instance, if the geodesic motions of particles in the two spacetimes significantly differ, the microstate geometries may be unable to be regarded as an alternative to the black hole. The main purpose of this paper is to study stable bound orbits in the microstate geometries, more precisely, to investigate numerically whether stable bound orbits of particles can exist in the microstate geometries with the same mass and angular momenta as the BMPV black holes.

In our analysis, focusing on asymptotically flat, stationary BPS solutions with biaxisymmetry and reflection symmetry in the five-dimensional ungauged minimal

[*]tomizawa@toyota-ti.ac.jp
[†]sryotaku@toyota-ti.ac.jp

supergravity, we regard motion of particles as a two-dimensional potential problem. As discussed for several BPS black holes in the same theory [30,31,33–35], one can replace a problem of whether there exist stable bound orbits for particles with a simple problem of whether the two-dimensional effective potential has a negative local minimum. First, we numerically show the existence of stable bound orbits for massive particles for the microstate geometries with three Gibbons-Hawking centers. Next, we numerically show that there can be stable bound orbits of massive and massless particles for the microstate geometries with five Gibbons-Hawking centers which have the same mass and angular momenta as the BMPV black holes. Moreover, we also study the five center solutions whose angular momenta are larger than the BMPV black holes.

The rest of the paper is organized as follows: In the following Sec. II, we briefly review the microstate geometries in the five-dimensional minimal supergravity. In Sec. III, we provide our formalism to show the existence of stable bound orbits. In Sec. IV, using the formalism, we discuss whether there are stable bound orbits for massive and massless particles. In Sec. V, we summarize our results and discuss possible generalizations of our analysis.

II. MICROSTATE GEOMETRIES

A. Solutions

We review the microstate geometries in the five-dimensional minimal ungauged supergravity (the five-dimensional Einstein-Maxwell theory with a Chern-Simons term) [38,40]. The metric and the gauge potential 1-form of the Maxwell field can be written as

$$ds^2 = -f^2(dt+\omega)^2 + f^{-1}ds_M^2, \tag{1}$$

$$A = \frac{\sqrt{3}}{2}\left[f(dt+\omega) - \frac{K}{H}(d\psi+\chi) - \xi\right], \tag{2}$$

where ds_M^2 is the metric of the Gibbons-Hawking space [41], which is written as

$$ds_M^2 = H^{-1}(d\psi+\chi)^2 + Hds_{\mathbb{E}^3}^2, \tag{3}$$

$$ds_{\mathbb{E}^3}^2 = dx^2+dy^2+dz^2 = dr^2 + r^2(d\theta^2+\sin^2\theta d\phi^2), \tag{4}$$

$$\chi = \sum_{i=1}^{n} h_i \frac{r\cos\theta - z_i}{r_i} d\phi, \tag{5}$$

$$H = \sum_{i=1}^{n} \frac{h_i}{r_i}. \tag{6}$$

Here, $r_i (i=1,\ldots,n)$ is the distance between $\boldsymbol{r} \coloneqq (x,y,z)$ and the ith point source $\boldsymbol{r}_i \coloneqq (0,0,z_i)$ of a harmonic function H on $\mathbb{E}^3$ and is defined as

$$r_i \coloneqq |\boldsymbol{r}-\boldsymbol{r}_i| = \sqrt{x^2+y^2+(z-z_i)^2} = \sqrt{r^2-2rz_i\cos\theta+z_i^2}. \tag{7}$$

The function f^{-1} and the 1-forms (ω,ξ) are written as

$$f^{-1} = H^{-1}K^2 + L, \tag{8}$$

$$\begin{aligned}\omega = &\left(H^{-2}K^3 + \frac{3}{2}H^{-1}KL + M\right)(d\psi+\chi) \\ &+ \left[\sum_{i,j=1(i\neq j)}^{n}\left(h_im_j + \frac{3}{2}k_il_j\right)\frac{r^2-(z_i+z_j)r\cos\theta+z_iz_j}{z_{ji}r_ir_j}\right. \\ &\left. - \sum_{i=1}^{n}\left(m_0h_i + \frac{3}{2}l_0k_i\right)\frac{r\cos\theta-z_i}{r_i} + c\right]d\phi,\end{aligned} \tag{9}$$

$$\xi = -\sum_{i=1}^{n} k_i \frac{r\cos\theta - z_i}{r_i} d\phi, \tag{10}$$

where the functions K, L, and M are harmonic functions on $\mathbb{E}^3$,

$$K = \sum_{i=1}^{n}\frac{k_i}{r_i}, \quad L = l_0 + \sum_{i=1}^{n}\frac{l_i}{r_i}, \quad M = m_0 + \sum_{i=1}^{n}\frac{m_i}{r_i}. \tag{11}$$

Since we assume that all point sources lie on the z axis, the solutions have three commuting Killing vectors $\partial/\partial t, \partial/\partial\psi$, and $\partial/\partial\phi$, and the coordinate has the ranges $-\infty < t < \infty$, $r > 0$, $0 \le \psi < 4\pi$, $0 \le \phi < 2\pi$, and $0 \le \theta \le \pi$.

As discussed in Refs. [38,42], asymptotic flatness requires the parameters to be subject to

$$\sum_{i=1}^{n} h_i = 1, \tag{12}$$

$$l_0 = 1, \tag{13}$$

$$c = \sum_{i,j=1(i\neq j)}^{n} \frac{h_im_j + \frac{3}{2}k_il_j}{z_{ij}}, \tag{14}$$

$$m_0 = -\frac{3}{2}\sum_{i=1}^{n} k_i. \tag{15}$$

From the requirements of regularity at $\boldsymbol{r} = \boldsymbol{r}_i (i=1,\ldots,n)$, the parameters $(k_{i\geq 1}, l_{i\geq 1}, m_{i\geq 1})$ must satisfy

$$l_i = -\frac{k_i^2}{h_i}, \tag{16}$$

$$m_i = \frac{k_i^3}{2h_i^2}. \tag{17}$$

Moreover, to ensure Lorentzian signature of the metric around the points $\boldsymbol{r} = \boldsymbol{r}_i (i = 1, \ldots, n)$, the inequalities

$$h_i^{-1} c_{1(i)} \coloneqq h_i + \sum_{j=1(j\neq i)}^{n} \frac{2k_i k_j + l_i h_j + h_i l_j}{|z_{ij}|} > 0 \tag{18}$$

must be satisfied, and from the absence of closed timelike curves around the points, they must also satisfy

$$h_i c_{2(i)} \coloneqq h_i m_0 + \frac{3}{2} k_i + \sum_{j=1(j\neq i)}^{n} \frac{h_i m_j - m_i h_j - \frac{3}{2}(l_i k_j - k_i l_j)}{|z_{ij}|} = 0. \tag{19}$$

In addition, the absence of orbifold singularities at $\boldsymbol{r} = \boldsymbol{r}_i (i = 1, \ldots, n)$ demands

$$h_i = \pm 1 (i = 1, \ldots, n). \tag{20}$$

B. Useful coordinates

In the work of the geodesic motion of particles, it is more convenient to use the coordinates (ρ, ϕ_1, ϕ_2) defined by

$$x = \rho \cos(\phi_1 - \phi_2), \qquad y = \rho \sin(\phi_1 - \phi_2),$$
$$\psi = \phi_1 + \phi_2, \qquad \phi = \phi_1 - \phi_2, \tag{21}$$

where (ϕ_1, ϕ_2) are the coordinates with 2π periodicity.

C. Three-center solutions

The solutions with three centers $(n = 3)$ and $(h_1, h_2, h_3) = (1, -1, 1)$ describe the simplest asymptotically flat, stationary, and biaxisymmetric microstate geometries, which have the four parameters (k_1, k_3, z_1, z_3), where we have set $k_2 = 0$ and $z_2 = 0$. Moreover, under the assumption of the reflection symmetry

$$z_3 = -z_1 =: a (> 0), \qquad k_3 = k_1, \tag{22}$$

the bubble equations (19) are simply written as

$$c_{2(1)} = -\frac{1}{2} c_{2(2)} = c_{2(3)} = \frac{k_1 [k_1^2 - 3a]}{2a} = 0, \tag{23}$$

which lead to

$$k_1 = 0, \qquad a = \frac{k_1^2}{3}. \tag{24}$$

Only the latter case can satisfy the inequalities (18), where $h_i c_{1(i)}$ $(i = 1, 2, 3)$ are computed as

$$h_1 c_{1(1)} = h_3 c_{1(3)} = 4, \qquad h_2 c_{1(2)} = 5. \tag{25}$$

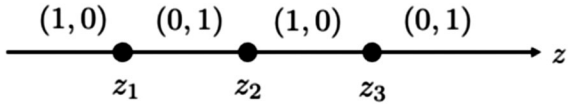

FIG. 1. Rod structure for the microstate geometries with three centers and $(h_1, h_2, h_3) = (1, -1, 1)$.

Therefore, for arbitrary nonzero k_1, this describes regular and causal solutions of asymptotically flat, stationary microstate geometries with the biaxisymmetry and reflection symmetry. The solutions were previously analyzed in Ref. [10].

The z axis of $\mathbb{E}^3$ in the Gibbons-Hawking space consists of the four intervals: $I_- = \{(x, y, z) | x = y = 0, z < z_1\}$, $I_i = \{(x, y, z) | x = y = 0, z_i < z < z_{i+1}\}$ $(i = 1, 2)$, and $I_+ = \{(x, y, z) | x = y = 0, z > z_3\}$. The rod structure of the three-center microstate geometries is displayed in Fig. 1.

Under the symmetric conditions (22) and gauge conditions $k_2 = 0$, $z_2 = 0$, the Arnowitt-Deser-Misner (ADM) mass, two ADM angular momenta, and the magnetic fluxes on I_i $(i = 1, 2)$ are written as, respectively,

$$M = \frac{\sqrt{3}}{2} Q = 6\pi k_1^2, \tag{26}$$

$$J_\psi = 3\pi k_1^3, \tag{27}$$

$$J_\phi = 0, \tag{28}$$

$$q[I_1] = -q[I_2] = \frac{\sqrt{3}}{2} k_1. \tag{29}$$

As discussed in Ref. [38], the squared angular momentum normalized by the mass is written as

$$j^2 = \frac{9}{8}. \tag{30}$$

This is larger than the BMPV black holes which have the range of $0 \leq j^2 < 1$.

D. Five-center solutions

The stationary, biaxisymmetric microstate geometries with five centers $(n = 5)$ and $(h_1, h_2, h_3, h_4, h_5) = (1, -1, 1, -1, 1)$ have the four parameters (k_1, k_2, z_1, z_2) under the reflection-symmetric conditions

$$k_5 = k_1, \quad k_4 = k_2, \quad z_5 = -z_1 =: a + b, \quad z_4 = -z_2 =: b \tag{31}$$

and the gauge conditions $k_3 = 0$, $z_3 = 0$. Thus, the conditions (19) are simplified as

$$2h_1 c_{2(1)} = 2h_5 c_{2(5)} = -3(k_1 + 2k_2) - \frac{k_1^3}{a + b} + \frac{(k_1 + k_2)^3}{a} + \frac{(k_1 + k_2)^3}{a + 2b} = 0, \tag{32}$$

$$2h_2c_{2(2)} = 2h_4c_{2(4)} = 3(2k_1 + 3k_2) - \frac{k_2^3}{b} - \frac{(k_1+k_2)^3}{a} - \frac{(k_1+k_2)^3}{a+2b} = 0, \quad (33)$$

$$h_3c_{2(3)} = -3(k_1+k_2) + \frac{k_1^3}{a+b} + \frac{k_2^3}{b} = 0, \quad (34)$$

where we note that Eqs. (32)–(34) are not independent due to the constraint equation $\sum_{i=1}^{5} h_i c_{2(1)} = 2h_1c_{2(1)} + 2h_2c_{2(2)} + h_3c_{2(3)} = 0$. Therefore, the solutions have only two independent parameters. If we regard a and b as the functions of k_1 and k_2 from Eqs. (32) and (34), the solutions are a two-parameter family for (k_1, k_2).

Furthermore, the parameters k_1 and k_2 must satisfy the inequalities (18), which are written as

$$h_1c_{1(1)} = h_5c_{1(5)} = 1 - \frac{k_1^2}{a+b} + \frac{(k_1+k_2)^2}{a} + \frac{(k_1+k_2)^2}{a+2b} > 0, \quad (35)$$

$$h_2c_{1(2)} = h_4c_{1(4)} = -1 + \frac{k_2^2}{b} + \frac{(k_1+k_2)^2}{a} + \frac{(k_1+k_2)^2}{a+2b} > 0, \quad (36)$$

$$h_3c_{1(3)} = 1 - \frac{2k_1^2}{a+b} + \frac{2k_2^2}{b} > 0, \quad (37)$$

with the inequalities $a > 0$, $b > 0$. In the below, we assume $k_1 \neq 0$ and $k_2 \neq 0$. As shown in Ref. [38], these inequalities are equivalent with

$$k_2/k_1 < -1, \quad -0.2063\ldots < k_2/k_1 < 0, \quad k_2/k_1 > 0. \quad (38)$$

The z of $\mathbb{E}^3$ in the Gibbons-Hawking space consists of the six intervals: $I_- = \{(x,y,z)|x = y = 0, z < z_1\}$, $I_i = \{(x,y,z)|x = y = 0, z_i < z < z_{i+1}\}(i = 1,\ldots,4)$ and $I_+ = \{(x,y,z)|x = y = 0, z > z_5\}$. The five-center microstate geometries have the rod structure displayed in Fig. 2.

For the solutions, the ADM mass, two ADM angular momenta the magnetic fluxes are computed as

$$M = \frac{\sqrt{3}}{2}Q = 6\pi(k_1^2 + 4k_1k_2 + 3k_2^2), \quad (39)$$

$$J_\psi = 3\pi(k_1^3 + 6k_1^2k_2 + 10k_1k_2^2 + 5k_2^3), \quad (40)$$

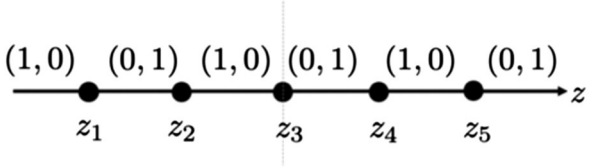

FIG. 2. Rod structure for the microstate geometries with five centers and $(h_1, h_2, h_3, h_4, h_5) = (1, -1, 1, -1, 1)$.

$$J_\phi = 0, \quad (41)$$

$$q[I_1] = -q[I_4] = \frac{\sqrt{3}}{2}(k_1+k_2), \quad q[I_2] = -q[I_3] = -\frac{\sqrt{3}}{2}k_2. \quad (42)$$

As discussed in Ref. [38], the squared angular momentum runs the range

$$j^2 > 0.841\ldots. \quad (43)$$

The biaxisymmetric and reflectionally symmetric microstate geometries with five centers can have the same angular momentum of the range $0.841\ldots < j^2 < 1$ as the BMPV black holes.

III. OUR FORMALISM

To study stable bound orbits, we regard the geodesic motion of massive and massless particles as a two-dimensional potential problem (see Ref. [30] for the details). The Hamiltonian of a free particle with mass m is written as

$$\mathcal{H} = g^{\mu\nu}p_\mu p_\nu + m^2, \quad (44)$$

where p_μ is the momentum such that $(p_t, p_{\phi_1}, p_{\phi_2}) = (-E, L_{\phi_1}, L_{\phi_2})$ are constants of motion. Then, the Hamiltonian can be rewritten as

$$\mathcal{H} = \frac{4f}{H\rho^2}(p_\rho^2 + p_z^2) + E^2\left(U + \frac{m^2}{E^2}\right). \quad (45)$$

The effective potential $U = U(\rho, z)$ is given by

$$U = g^{tt} + g^{\phi_1\phi_1}l_{\phi_1}^2 + g^{\phi_2\phi_2}l_{\phi_2}^2 - 2g^{t\phi_1}l_{\phi_1} - 2g^{t\phi_2}l_{\phi_2} + 2g^{\phi_1\phi_2}l_{\phi_1}l_{\phi_2} \quad (46)$$

$$= \frac{1}{4(K^2+HL)}[-3K^2L^2 + 8K^3M + 12HKLM - 4HL^3 + 4H^2M^2 + (4K^3 + 6HKL + 4H^2M)(l_{\phi_1} + l_{\phi_2}) + H^2(l_{\phi_1} + l_{\phi_2})^2] + \frac{[-2\hat{\omega}_\phi + (l_{\phi_1} + l_{\phi_2})\chi_\phi + (l_{\phi_2} - l_{\phi_1})]^2}{4(K^2+HL)\rho^2}, \quad (47)$$

where two angular momenta (L_{ϕ_1}, L_{ϕ_2}) are normalized by the energy E as $l_{\phi_1} \coloneqq L_{\phi_1}/E$ and $l_{\phi_2} \coloneqq L_{\phi_2}/E$. Thus, particles move on the two-dimensional space (ρ, z) in the two-dimensional potential $U(\rho, z)$, satisfying the Hamiltonian constraint $\mathcal{H} = 0$. The allowed regions of the motions for massive and massless particles correspond to $U \leq -m^2/E^2$ and $U \leq 0$, respectively. If U has a negative local minimum for given (l_{ϕ_1}, l_{ϕ_2}), stable bound orbits exist for massive particles at the point or in the neighborhood of the point, and furthermore if the curve $U = 0$ in the (ρ, z) plane or the region surrounded with the

$U = 0$ curve and the z axis is closed, stable bound orbits exist even for massless particles.

IV. STABLE BOUND ORBITS

A. Three-center solutions

To see whether there exist stable bound orbits in the microstate geometries for $n = 3$, let us focus on the simple case of $l_{\phi_2} = 0$. For the three-center solutions, the z axis is composed of the four intervals, $I_- = \{(\rho, z)|\rho = 0, z < z_1\}$, $I_1 = \{(\rho, z)|\rho = 0, z_1 < z < z_2\}$, $I_2 = \{(\rho, z)|\rho = 0, z_2 < z < z_3\}$, and $I_+ = \{(\rho, z)|\rho = 0, z > z_3\}$. As was previously shown in [30], it should be noted that only particles with the angular momentum of $l_{\phi_2} = 0$ can move on I_1 and I_+ (because I_+ and I_1 correspond to the fixed points of the Killing isometry $v_2 \coloneqq \partial/\partial\phi_2$), and hence only particles with the angular momentum of $J \coloneqq p_\mu v_2^\mu = L_{\phi_2} = 0 (l_{\phi_2} = 0)$ can move on the z axis, whereas (because U diverges) on I_- and I_2 the particles cannot move. It can be shown from the entirely similar discussion that on I_- and I_2 only particles with the angular momenta of $l_{\phi_1} = 0$ are allowed to move there.

Figure 3 displays the typical contour plots of U in the (ρ, z) plane for the parameter setting $(k_1, k_2, k_3) = (\sqrt{3}, 0, \sqrt{3})$,

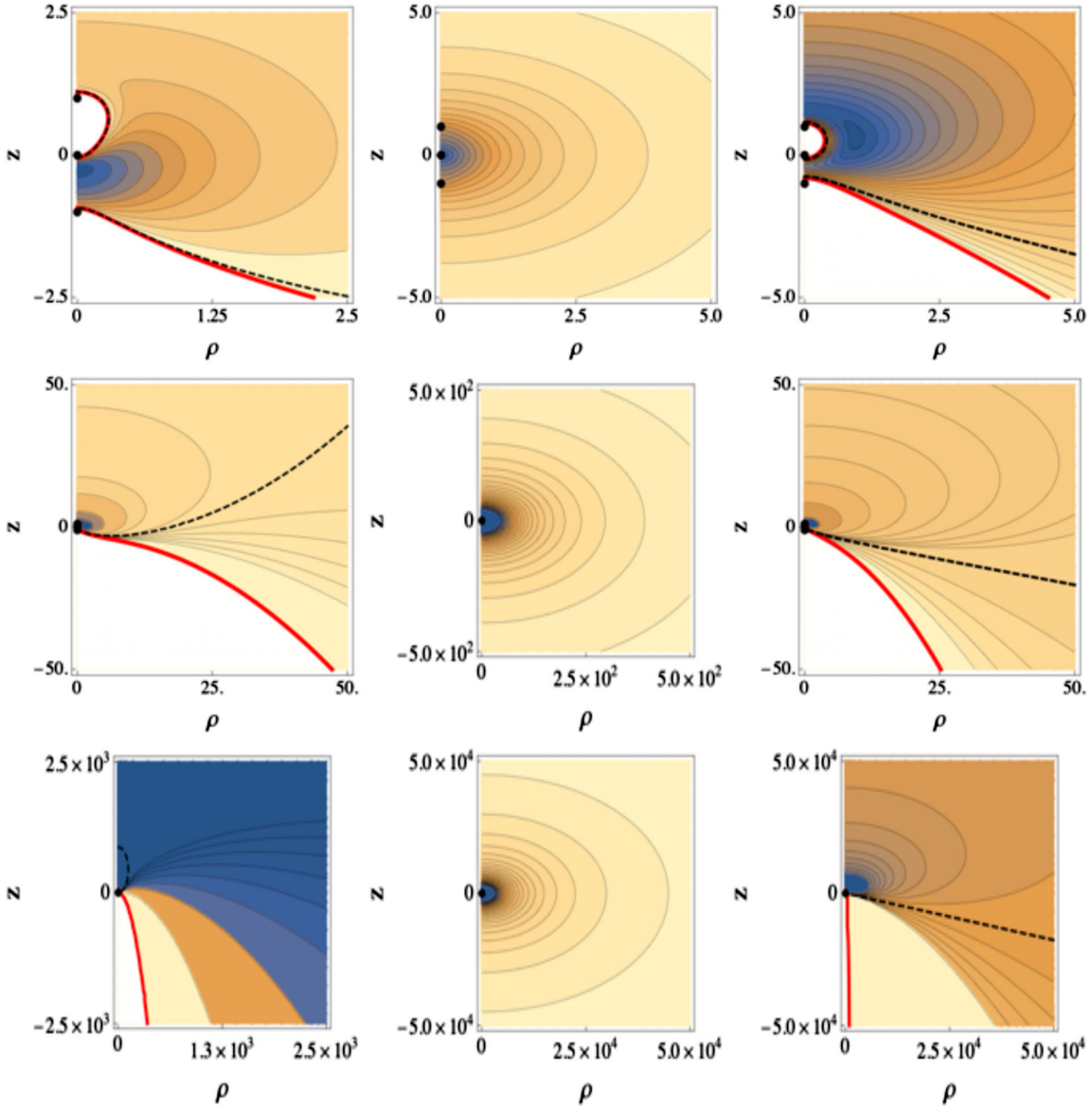

FIG. 3. The figures show the contours of the potential U under the parameter setting $(k_1, k_2, k_3) = (\sqrt{3}, 0, \sqrt{3})$ and $(z_1, z_2, z_3) = (-1, 0, 1)$. The left, middle, and right figures correspond to the angular momenta $(l_{\phi_1}, l_{\phi_2}) = (-7, 0), (0, 0), (4, 0)$, respectively, and the upper, middle, and lower figures differ only in the scales of the vertical and horizontal axes. The bold solid curves and the dashed curves denote $U = 0$ and $U = -1$, respectively, and the white regions denote the forbidden regions of $U > 0$ where massive and massless particles cannot move. The black circles correspond to the centers at $(\rho, z) = (0, z_i)$ $(i = 1, 2, 3)$.

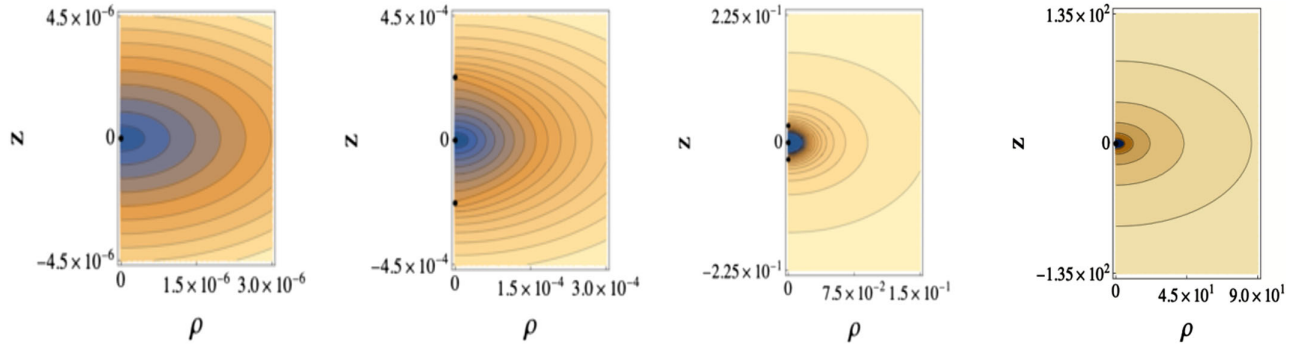

FIG. 4. The figures show the contours of the potential U under the parameter setting $(k_1, k_2, k_3, k_4, k_5) = (1, -0.192, 0, -0.192, 1)$ and angular momenta $(l_{\phi_1}, l_{\phi_2}) = (0, 0)$, where $j^2 \simeq 0.919$ and $(a, b) \simeq (0.0296, 0.000227)$. The solid curves denote the contours $U = \text{constant}(< 0)$, and the black circles correspond to the centers at $(\rho, z) = (0, z_i)(i = 1, \ldots, 5)$.

which corresponds to the solutions with $j^2 = 9/8$ and $(z_1, z_2, z_3) = (-1, 0, 1)$, where it should be noted that the upper, middle, and lower figures differ only in the scales of the horizontal axis and vertical axis, and the left, middle, and right figures correspond to the angular momenta of particles $(l_{\phi_1}, l_{\phi_2}) = (-7, 0), (0, 0), (4, 0)$, respectively. In these figures, the red curves denote the contours $U = 0$, which we call $U = 0$ curves. For each case of $(l_{\phi_1}, l_{\phi_2}) = (-7, 0), (4, 0)$, the $U = 0$ curve intersects with I_1 and I_+ on the z axis so that it makes a closed region surrounded with the z axis. Since $U > 0 (< 0)$ inside (a little outside) the $U = 0$ curve, there are not stable bound orbits for massless particles. It can be seen from these figures that in each case, U has a negative local minimum outside the $U = 0$ curve, i.e., there are stable bound orbits for massive particles. In particular, for $(l_{\phi_1}, l_{\phi_2}) = (-7, 0)$, the stable bound orbit at the local minimum is circular because U has the local minimum on I_1, where massive particles move along $\partial/\partial\phi_1$. On the other hand, it can be shown from the three middle figures that for $(l_{\phi_1}, l_{\phi_2}) = (0, 0)$, U does not have a $U = 0$ curve and has a local minimum at the center (0,0). Therefore, stable bound orbits do not exist for massless particles but exist for massive particles. Moreover, U is monotonically increasing at large distances and $U \to -1$ at $r \to \infty$; the stable bound orbits exist for massive particles even at infinity.

B. Five-center solutions

For the five centers, the z axis of $\mathbb{E}^3$ in the Gibbons-Hawking space consists of the six intervals, $I_- = \{(x, y, z) | x = y = 0, z < z_1\}$, $I_i = \{(x, y, z) | x = y = 0, z_i < z < z_{i+1}\} (i = 1, \ldots, 4)$, and $I_+ = \{(x, y, z) | x = y = 0, z > z_5\}$. As was previously discussed in [30], only particles with the angular momentum of $l_{\phi_2} = 0$ can move on I_1, I_3, I_+ but cannot move on I_-, I_2 and I_4. Similarly, only particles with the angular momenta of $l_{\phi_1} = 0$ are allowed to move on I_-, I_2 and I_4 but cannot move on I_1, I_3, and I_+. Here, as typical examples, we study two cases of $j^2 \simeq 0.919$ and $j^2 \simeq 14.8$ for particles with $l_{\phi_2} = 0$:

1. $j^2 \simeq 0.919$

Figure 4 displays the contour plots of U for particles with zero angular momenta, $(l_{\phi_1}, l_{\phi_2}) = (0, 0)$ under the parameter setting $(k_1, k_2, k_3, k_4, k_5) = (1, -0.192, 0, -0.192, 1)$, which corresponds to the solutions with $j^2 \simeq 0.919$ and $(a, b) \simeq (0.0296, 0.000227)$, where it should be noted that the four figures differ only in the scales of the horizontal axis and vertical axis. It can be shown from these figures that for $(l_{\phi_1}, l_{\phi_2}) = (0, 0)$, U is negative (hence U does not have a $U = 0$ curve) and has a local minimum at the center (0,0). Therefore, stable bound orbits do not exist for massless particles but exist for massive particles. In particular, massive particles at (0,0) remain at rest. Moreover, U is monotonically increasing at large distances and $U \to -1$ at $r \to \infty$, stable bound orbits exist for massive particles even at infinity.

Next, we consider the case of $l_{\phi_1} \neq 0, l_{\phi_2} = 0$ under the same parameter setting as the above case. Figure 5 displays the typical contour plots of U for particles with nonzero angular momenta, where we plot the case $(l_{\phi_1}, l_{\phi_2}) = (-14, 0)$ as an example. It should be noted here that each figure differs only in the scales of the horizontal axis and vertical axis. For particles with $(l_{\phi_1}, l_{\phi_2}) = (-14, 0)$, there are four $U = 0$ curves: (i) the inner $U = 0$ curve which surrounds the two centers at $z = z_2 (\simeq -0.000227)$ and $z = z_3 (= 0)$ and intersects with I_1 and I_3 [the $U = 0$ curve in the upper left figure and the lower $U = 0$ curves in the upper middle and upper right figures], (ii) the inner $U = 0$ curve which surrounds the two centers at $z = z_4 (\simeq 0.000227)$ and $z = z_5 (\simeq 0.0298)$ and intersects with I_3 and I_+ [the upper $U = 0$ curves in the upper middle and the upper right figures, the $U = 0$ curve in the middle left figure, the upper $U = 0$ curve in the middle figure, and the smaller $U = 0$ curve in the middle right figure], (iii) the intermediate $U = 0$ curve which surrounds the two inner $U = 0$ curves with the z axis, and intersects with I_1 and I_+ [the larger $U = 0$ curve in the middle right figure], and (iv) the outer $U = 0$ curve which surrounds the intermediate $U = 0$ curve and intersects with only I_+ [the $U = 0$

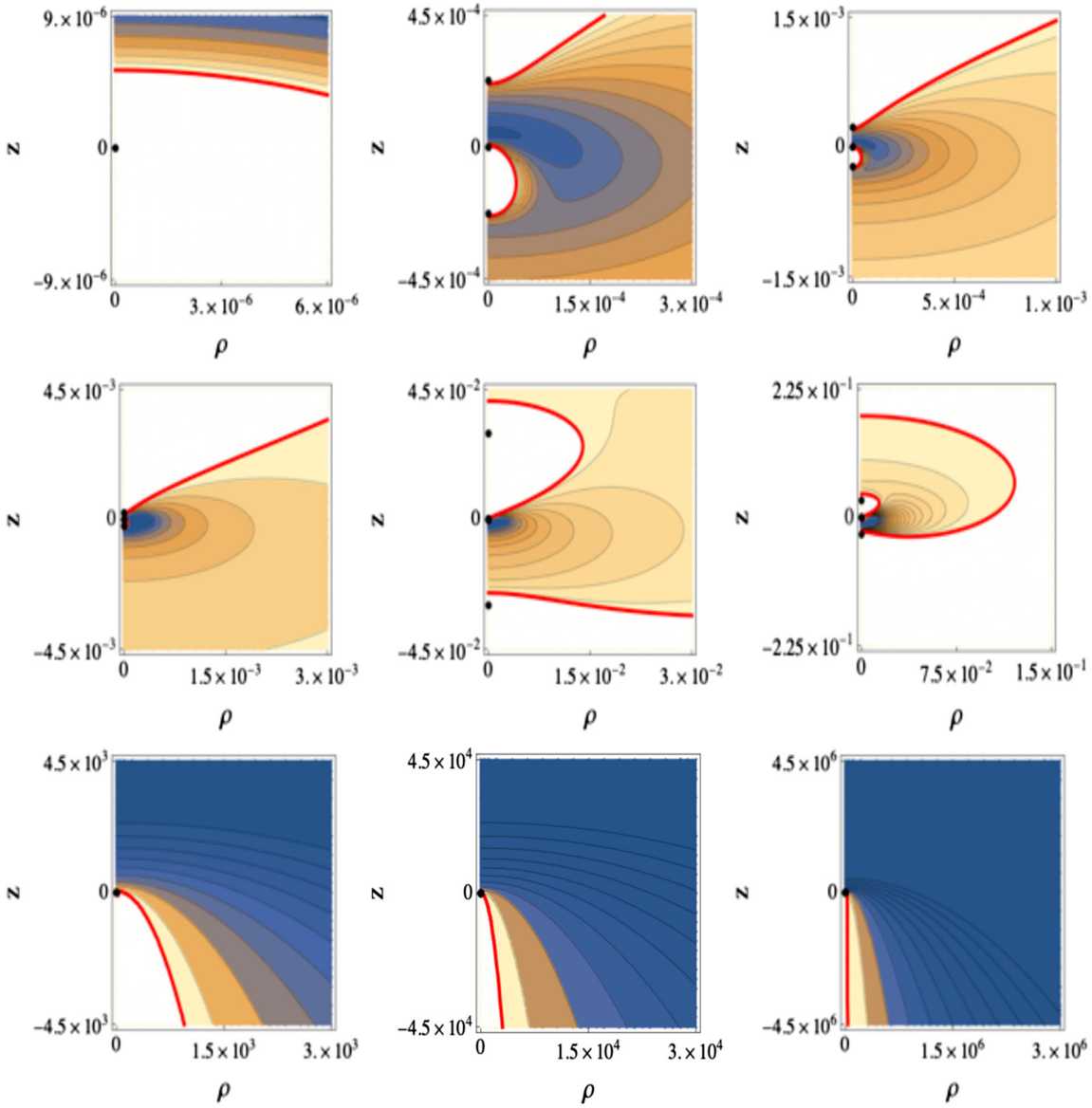

FIG. 5. The figures show the contours of the potential U under the parameter setting $(k_1, k_2, k_3, k_4, k_5) = (1, -0.192, 0, -0.192, 1)$ and angular momenta $(l_{\phi_1}, l_{\phi_2}) = (-14, 0)$, where $j^2 \simeq 0.919$ and $(a, b) \simeq (0.0296, 0.000227)$. The bold solid curves denote $U = 0$ and the white regions denote the forbidden regions of $U > 0$ where massive and massless particles cannot move. The black circles correspond to the centers at $(\rho, z) = (0, z_i)(i = 1, \ldots, 5)$.

curves in the three lower figures]. It can be seen from these figures that $U > 0 (< 0)$ inside (a little outside) the inner $U = 0$ curves, $U < 0 (> 0)$ a little inside (a little outside) the intermediate $U = 0$ curve, and $U > 0 (< 0)$ a little inside (outside) the outer $U = 0$ curve. Thus, U has two negative local minima in the closed region surrounded with the two inner $U = 0$ curves, the intermediate $U = 0$ curve and the z axis. Therefore, there are stable bound orbits for both massive and massless particles in the region. Moreover, a stable circular orbit exists for massive particles at the local minimum of U, which is on I_3 and hence particles at the point must move along $\partial/\partial\phi_1$.

2. $j^2 \simeq 14.8$

Finally, we study the case $j^2 \simeq 14.8$ as the much larger example than the upper bounds for the angular momenta of the BMPV black holes. Figure 6 shows the contours of U for $(l_{\phi_1}, l_{\phi_2}) = (0, 0)$ and the parameters $(k_1, k_2, k_3, k_4, k_5) = (1, -1.01, 0, -1.01, 1)$, which correspond to the solutions with $j^2 \simeq 14.8$ and $(a, b) \simeq (4.83 \times 10^{-7}, 1.01)$, where the figures differ only in the scales of the horizontal axis and the vertical axis. As can be seen from these figures, U does not have a $U = 0$ curve, and hence stable bound orbits do not exist for massless particles. On the other hand, it can be seen from the middle figure that U has two negative local

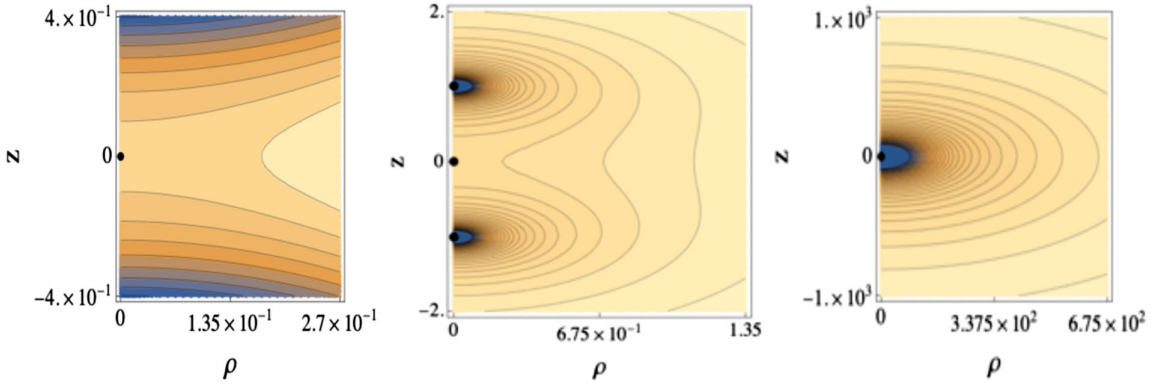

FIG. 6. The figures show the contours of the potential U under the parameter setting $(k_1, k_2, k_3, k_4, k_5) = (1, -1.01, 0, -1.01, 1)$ and angular momenta $(l_{\phi_1}, l_{\phi_2}) = (0, 0)$, where $j^2 \simeq 14.8$ and $(a, b) \simeq (4.83 \times 10^{-7}, 1.01)$.

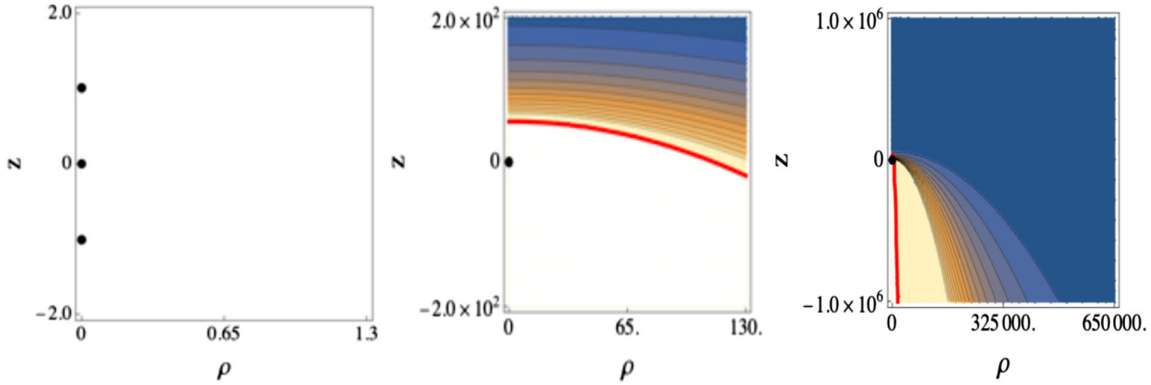

FIG. 7. The figures show the contours of the potential U under the parameter setting $(k_1, k_2, k_3, k_4, k_5) = (1, -1.01, 0, -1.01, 1)$ and angular momenta $(l_{\phi_1}, l_{\phi_2}) = (-15, 0)$, where $j^2 \simeq 14.8$ and $(a, b) \simeq (4.83 \times 10^{-7}, 1.01)$.

minima at the z axis, so that stable bound orbits exist for massive particles.

Figure 7 shows the contours of U for $(l_{\phi_1}, l_{\phi_2}) = (-15, 0)$ under the same parameter setting as the above. As can be seen from these figures, there exists the single nonclosed $U = 0$ curve which intersects with I_+ and extends to infinity. $U > 0 (< 0)$ inside (outside) the $U = 0$ curve, and U does not has a local minimum, i.e., bound orbits do not exist for massive/massless particles. Moreover, particles coming in from infinity cannot enter inside the $U = 0$ curve, which also occurs for the over-rotating BMPV black holes (so-called repulsons).

V. SUMMARY AND DISCUSSION

We have investigated the existence of stable bound orbits for the massive and massless particles moving in the simplest microstate geometry backgrounds with reflection symmetry (three-center solutions and five-center solutions) in the bosonic sector of the five-dimensional minimal supergravity. In our analysis, reducing the motion of particles to a two-dimensional potential problem, we have plotted the contours of the potential. More specially, we have shown the following points:

(i) We have numerically shown that the three-center microstate geometries, which must have larger angular momenta than the BMPV black holes, admit the existence of stable bound for massive particles near the three-center orbits but also even at infinity. This is quite different from the geodesic behaviors in the five-dimensional black hole backgrounds. We could not confirm the existence of stable bound orbits for massless particles. We have found numerically that there is such a finite region near the centers that massive particles with nonzero angular momenta coming in from infinity cannot reach (the closed white regions in the upper left and upper right figures of Fig. 3). This resembles the repulson behavior of the BMPV black holes with over-rotation ($j^2 > 1$) [43,44], in which case since the horizon area becomes imaginary, hence ill defined; it simply becomes a smooth timelike hypersurface (called a pseudohorizon). Though the geodesics are complete in such a spacetime, surprisingly,

massive and massless particles cannot enter inside the pseudohorizon.

(ii) We have compared the five-center solutions and the BMPV black holes with the same mass and two angular momenta. In the under-rotating BMPV black hole background ($0 < j^2 < 1$), stable bound orbits do not exist outside the horizon for massive and massless particles, whereas in the microstate geometries, they exist (near the five Gibbons-Hawking centers) for both massive and massless particles. In addition, the solutions also admit the repulson behavior of the over-rotating BMPV black holes since particles with nonzero angular momenta cannot enter inside the two $U = 0$ curves (see the closed white regions in the upper middle and middle figures of Fig. 5). Moreover, we have investigated the five-center microstate geometries (with reflectional symmetry) having angular momenta larger than the BMPV black holes. At least, numerically, we could confirm the existence of stable bound orbits for massive particles with zero angular momenta (not only near the centers but also at infinity) but could not for massless particles. Moreover, particles with nonzero angular momenta cannot reach near the Gibbons-Hawking centers (see Fig. 7).

It is an interesting issue to analyze more general microstate solutions with a larger number of centers or without reflectional symmetry of centers. These deserve our future work.

ACKNOWLEDGMENTS

We thank Takahisa Igata for useful discussion and comments. R. S. was supported by JSPS KAKENHI Grant No. JP18K13541. S. T. was supported by JSPS KAKENHI Grants No. 17K05452 and No. 21K03560.

[1] O. Lunin and S. D. Mathur, AdS/CFT duality and the black hole information paradox, Nucl. Phys. **B623**, 342 (2002).
[2] J. M. Maldacena and L. Maoz, Desingularization by rotation, J. High Energy Phys. 12 (2002) 055.
[3] V. Balasubramanian, J. de Boer, E. Keski-Vakkuri, and S. F. Ross, Supersymmetric conical defects: Towards a string theoretic description of black hole formation, Phys. Rev. D **64**, 064011 (2001).
[4] O. Lunin, J. M. Maldacena, and L. Maoz, Gravity solutions for the D1-D5 system with angular momentum, arXiv: hep-th/0212210.
[5] O. Lunin, Adding momentum to D1-D5 system, J. High Energy Phys. 04 (2004) 054.
[6] S. Giusto, S. D. Mathur, and A. Saxena, Dual geometries for a set of 3-charge microstates, Nucl. Phys. **B701**, 357 (2004).
[7] S. Giusto, S. D. Mathur, and A. Saxena, 3-charge geometries and their CFT duals, Nucl. Phys. **B710**, 425 (2005).
[8] S. Giusto and S. D. Mathur, Geometry of D1-D5-P bound states, Nucl. Phys. **B729**, 203 (2005).
[9] I. Bena and N. P. Warner, Bubbling supertubes and foaming black holes, Phys. Rev. D **74**, 066001 (2006).
[10] G. W. Gibbons and N. P. Warner, Global structure of five-dimensional fuzzballs, Classical Quantum Gravity **31**, 025016 (2014).
[11] A. Saxena, G. Potvin, S. Giusto, and A. W. Peet, Smooth geometries with four charges in four dimensions, J. High Energy Phys. 04 (2006) 010.
[12] K. Skenderis and M. Taylor, The fuzzball proposal for black holes, Phys. Rep. **467**, 117 (2008).
[13] V. Balasubramanian, J. de Boer, S. El-Showk, and I. Messamah, Black holes as effective geometries, Classical Quantum Gravity **25**, 214004 (2008).
[14] B. D. Chowdhury and A. Virmani, Modave lectures on fuzzballs and emission from the D1-D5 system, arXiv: 1001.1444.
[15] S. D. Mathur, The fuzzball proposal for black holes: An elementary review, Fortschr. Phys. **53**, 793 (2005).
[16] S. D. Mathur, The quantum structure of black holes, Classical Quantum Gravity **23**, R115 (2006).
[17] S. D. Mathur, Fuzzballs and the information paradox: A summary and conjectures, arXiv:0810.4525.
[18] A. Einstein, Demonstration of the non-existence of gravitational fields with a non-vanishing total mass free of singularities, Univ. Nac. Tucuman. Revista A **2**, 5 (1941), https://www.jnorman.com/pages/books/43311/albert-einstein/demonstration-of-the-non-existence-of-gravitational-elds-with-a-non-vanishing-total-mass-free-of.
[19] A. Einstein and W. Pauli, On the non-existence of regular stationary solutions of relativistic field equations, Ann. Math. **44**, 131 (1943).
[20] P. Breitenlohner, D. Maison, and G. W. Gibbons, Four-dimensional black holes from Kaluza-Klein theories, Commun. Math. Phys. **120**, 295 (1988).
[21] B. Carter, Mathematical foundations of the theory of relativistic stellar and black hole configurations, in *Gravitation in Astrophysics: Cargese 1986*, edited by B. Carter and J. Hartle, Nato ASI Series B: Physics Vol. 156 (Plenum, New York, 1986).
[22] F. R. Tangherlini, Schwarzschild field in n dimensions and the dimensionality of space problem, Nuovo Cimento **27**, 636 (1963).
[23] D. C. Wilkins, Bound geodesics in the Kerr metric, Phys. Rev. D **5**, 814 (1972).
[24] V. P. Frolov and D. Stojkovic, Particle and light motion in a space-time of a five-dimensional rotating black hole, Phys. Rev. D **68**, 064011 (2003).

[25] V. Diemer, J. Kunz, C. Lämmerzahl, and S. Reimers, Dynamics of test particles in the general five-dimensional Myers-Perry spacetime, Phys. Rev. D **89**, 124026 (2014).
[26] T. Igata, Stable bound orbits in six-dimensional Myers-Perry black holes, Phys. Rev. D **92**, 024002 (2015).
[27] T. Igata, H. Ishihara, and Y. Takamori, Stable bound orbits around black rings, Phys. Rev. D **82**, 101501 (2010).
[28] T. Igata, H. Ishihara, and Y. Takamori, Chaos in geodesic motion around a black ring, Phys. Rev. D **83**, 047501 (2011).
[29] T. Igata, H. Ishihara, and Y. Takamori, Stable bound orbits of massless particles around a black ring, Phys. Rev. D **87**, 104005 (2013).
[30] S. Tomizawa and T. Igata, Stable bound orbits around a supersymmetric black lens, Phys. Rev. D **100**, 124031 (2019).
[31] S. Tomizawa and T. Igata, Stable bound orbits in black lens backgrounds, Phys. Rev. D **102**, 124079 (2020).
[32] K. Nakashi and T. Igata, Innermost stable circular orbits in the Majumdar-Papapetrou dihole spacetime, Phys. Rev. D **99**, 124033 (2019).
[33] T. Igata and S. Tomizawa, Stable circular orbits in higher-dimensional multi-black hole spacetimes, Phys. Rev. D **102**, 084003 (2020).
[34] T. Igata and S. Tomizawa, Stable circular orbits in caged black hole spacetimes, Phys. Rev. D **103**, 084011 (2021).
[35] S. Tomizawa and T. Igata, Stable circular orbits in Kaluza-Klein black hole spacetimes, Phys. Rev. D **103**, 124004 (2021).
[36] F. C. Eperon, H. S. Reall, and J. E. Santos, Instability of supersymmetric microstate geometries, J. High Energy Phys. 10 (2016) 031.
[37] F. C. Eperon, Geodesics in supersymmetric microstate geometries, Classical Quantum Gravity **34**, 165003 (2017).
[38] S. Tomizawa, Lower bound for angular momenta of microstate geometries in five dimensions, Phys. Rev. D **104**, 084022 (2021).
[39] J. C. Breckenridge, R. C. Myers, A. W. Peet, and C. Vafa, D-branes and spinning black holes, Phys. Lett. B **391**, 93 (1997).
[40] J. P. Gauntlett, J. B. Gutowski, C. M. Hull, S. Pakis, and H. S. Reall, All supersymmetric solutions of minimal supergravity in five-dimensions, Classical Quantum Gravity **20**, 4587 (2003).
[41] G. W. Gibbons and S. W. Hawking, Gravitational multi-instantons, Phys. Lett. B **78**, 430 (1978).
[42] S. Tomizawa and M. Nozawa, Supersymmetric black lenses in five dimensions, Phys. Rev. D **94**, 044037 (2016).
[43] G. W. Gibbons and C. A. R. Herdeiro, Supersymmetric rotating black holes and causality violation, Classical Quantum Gravity **16**, 3619 (1999).
[44] V. Diemer and J. Kunz, Supersymmetric rotating black hole spacetime tested by geodesics, Phys. Rev. D **89**, 084001 (2014).